



---

# QUANTUM INTERNET ALLIANCE

# **D3.2 Report on interface to practical ground-to- satellite networks**

## Document History

Revision Nr	Description	Author	Review	Date
V1	Final version	Anders S. Sørensen, Anton Lauenborg Andersen, Eleni Diamanti, David Elkouss, Matteo Schiavon, Raja Yehia, Tim Coopmans		18 May 2021

*This project has received funding from the European Union's Horizon 2020 research and innovation programme under grant agreement No 820445.*

*The opinions expressed in this document reflect only the author's view and in no way reflect the European Commission's opinions. The European Commission is not responsible for any use that may be made of the information it contains.*

# Index

<b>1. Abstract</b>	<b>6</b>
<b>2. Keyword list</b>	<b>6</b>
<b>3. Acronyms &amp; Abbreviations</b>	<b>6</b>
<b>4. Part 1: Real-world satellite-ground link simulation</b>	<b>7</b>
<b>4.1 Introduction</b>	<b>7</b>
<b>4.2 Quantum key distribution through a single satellite node</b>	<b>8</b>
4.2.1 Channel model	8
4.2.2 Verifying correctness of the simulation code	9
4.2.3 Parameter study	10
4.2.4 Application to a simplified real-world scenario	12
<b>4.3 Conclusion</b>	<b>14</b>
<b>4.4 References</b>	<b>14</b>
<b>5. Part 2: Satellite-based communication with quantum memories</b>	<b>15</b>
<b>5.1 Introduction</b>	<b>15</b>
<b>5.2 Physical systems considered</b>	<b>16</b>
5.2.1 Satellite Link	16
5.2.2. Photon sources	17
5.2.3 Quantum emitters	17
5.2.4 Ensemble based memories	18
5.2.5 Photon scattering gates	19
<b>5.3 Applications for QKD</b>	<b>20</b>
5.3.1 Direct downlink	21
5.3.2 Ensemble downlink	21
5.3.3 Emitter downlink	22
5.3.4 Emitter uplink	23



<b>5.4 Entanglement distribution for applications</b>	<b>24</b>
5.4.1 Direct downlink	24
5.4.2 Memory assisted, ensemble based	25
5.4.3 Memory assisted, emitter based	26
<b>5.5 Conclusion</b>	<b>26</b>
<b>5.6 References</b>	<b>27</b>

# 1. Abstract

This report is divided in two parts that are considering short and long-term aspects of ground-satellite quantum communication networks, respectively.

In the first part, we report on computer simulations of secret key generation rates between two points on Earth (Paris and Delft) through a single satellite. In order to carry the simulations, we have implemented a realistic model of the transmission loss of photons through free space. This model was integrated in the NetSquid simulator for quantum networks, which was used for our analysis of the specific link scenario. This work is the first step towards a computer simulation of a large-scale terrestrial-space quantum network.

In the second part, we consider space-based quantum communication as an alternative to the approach pursued within the Quantum Internet alliance (QIA), namely long-distance quantum communication by exploiting quantum memories to construct quantum repeaters. Space based quantum communication currently holds the record for the long-distance quantum communication. The current satellite approach, however, only achieves a limited communication rate and does not allow for storage of entanglement, which is required for advanced quantum internet applications. We show here that merging the satellite-based approach with quantum memories can allow for a substantial increase in the quantum communication rate. We theoretically explore various methods to interface satellite-based quantum communication with quantum memories. We derive the minimal requirements for the memory performance, in terms of speed and coherence time, in order to exploit the memories for advanced entanglement-based protocols and boost the communication rate beyond what is achievable without memories. The requirements for this are challenging but not beyond reach of memories currently explored within QIA.

# 2. Keyword list

Quantum communication, quantum memories, satellite communication, quantum key distribution, quantum repeaters, entanglement distribution, free-space channel model.

# 3. Acronyms & Abbreviations

<b>DoA</b>	Description of Action
<b>EC</b>	European Commission
<b>WP</b>	Work Package
<b>MPQ</b>	Max Planck Institute for Quantum optics
<b>QIA</b>	Quantum Internet Alliance
<b>PDTC</b>	Probability Distribution of the Transmission Coefficient
<b>QKD</b>	Quantum Key Distribution
<b>SPDC</b>	Spontaneous Parametric Down Conversion

## 4. Part 1: Real-world satellite-ground link simulation

### 4.1 Introduction

The connection of quantum nodes at distant places is a fundamental point for a future global Quantum Internet. A crucial point for a quantum network consists of sharing the entanglement between different nodes. This task, however, is particularly challenging in the case of nodes placed at long distances, due to the fact that quantum states cannot be copied or amplified and are therefore very sensitive to channel losses.

Two main strategies are being investigated for distributing entanglement between distant nodes. The first one consists of a direct transfer of the entangled states between the different nodes, using either an optical fiber or a free-space channel. The second one exploits the entanglement swapping protocol in intermediate nodes, that act therefore as quantum repeaters. Since both quantum channels and quantum repeaters have a finite efficiency, it is necessary to find a way to evaluate the different strategies for entanglement distribution.

This evaluation requires a viable simulation of the different blocks of an entanglement distribution network. The Network Simulator for Quantum Information using Discrete events (NetSquid) provides a high-level framework for the simulation of quantum networks, where the different components can be added like lego blocks to construct complex systems.

This part of the deliverable is focused on the implementation of one of these blocks, i.e., the free-space quantum channel. Compared to the fiber channel, which is characterized by a fixed value of the transmittance, the free-space channel is controlled by atmospheric turbulence, which is an inherently random process and requires a statistical description of its properties. However, since the attenuation of the atmosphere is much lower than that of an optical fiber, the losses in this channel are mostly due to diffraction, they are therefore quadratic with distance and not exponential. For this reason, the free-space channel is thought to be one of the most promising tools for long distance entanglement distribution.

The free-space quantum channel is implemented in an open source NetSQUID snippet, called *netsquid-freespace*, that can be found on GitHub [1]. The repository contains also a first implementation of the utilities for the calculation of the varying channel parameters along the satellite orbit. Since this work is still on a preliminary stage, it will not be further described in this report.

## 4.2 Quantum key distribution through a single satellite node

We employ computer simulations to investigate quantum key distribution (QKD) between two nodes on earth (called 'Alice' and 'Bob') through an intermediate node in space. The key component that is different from a fully fiber-based setup is that the photons, the carriers of quantum information, are transmitted through free space. First, we will detail a theoretical model of the free-space channel and validate our code implementation of it. Next, we use our implementation to study the influence of properties of the setup (e.g. size of the telescope) on the rate at which secret keys can be obtained between Alice and Bob. Finally, we study the three-node QKD scenario and obtain the achievable raw key rate between two ground stations, Paris and Delft, who receive entanglement from a satellite.

### 4.2.1 Channel model

Since atmospheric turbulence is a very complex phenomenon, the realisation of a model for it requires a choice of the effects that mostly affect the transmission. The model proposed by Vasylyev et al. [2] presents a rigorous treatment of beam wandering effects, one of the leading causes of losses in the free-space channel. Its main advantage lies in an analytical formulation of the probability distribution of the transmission coefficient (PDTC), a feature exploited to provide a computationally efficient software implementation of the model. The model has also been applied recently to the satellite-to-ground channel [3]. A most complete model of atmospheric propagation for the satellite-to-ground case is described in Vasylyev et al. [4]. Its much higher complexity, however, makes it not very suitable for an implementation in NetSquid.

The current implementation takes into consideration two possible configurations for this channel, the ground-to-ground free space one (**class FreeSpaceLossModel**) and the satellite-to-ground one (**class FixedSatelliteLossModel**). The main difference lies in the fact that, while in the ground-to-ground channel all the propagation happens in the atmosphere, in the satellite-to-ground one only the last 10 km are affected by it. Since the effects of beam wandering depend mostly on the size of the beam at the beginning of the propagation in the atmosphere, their incidence is less important for the satellite-to-ground case than for the ground-to-ground one. In the satellite-to-ground case, on the other hand, the effects of pointing errors are more important, and must be added to the atmospheric beam wandering.

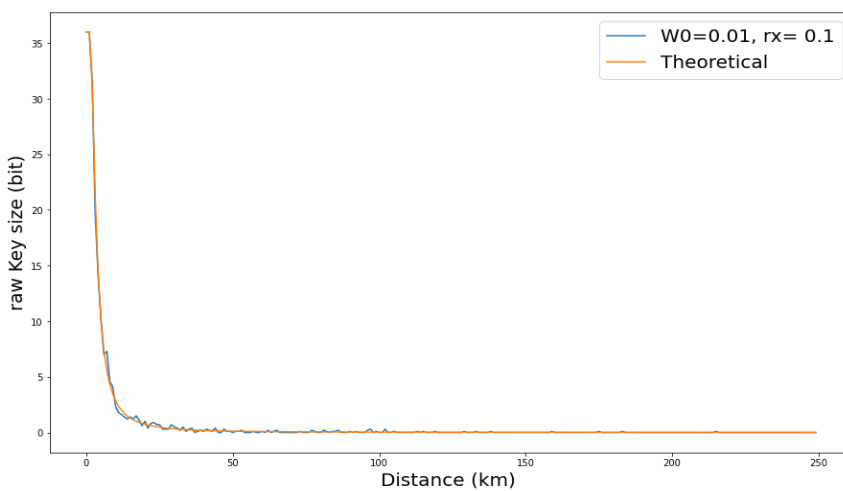
The parameters necessary to physically describe the channel are the size of the transmitting and receiving stations and the properties of the atmosphere and the pointing system. The transmitter is characterized by the beam waist **W0** in the ground-to-ground case and by the transmittance half-divergence **txDiv** for the satellite-to-ground case. This choice is due to the different conventions normally used in ground and space experiments for characterizing the transmitted beam. The relationship between these two parameters depends on the **wavelength** of the radiation used in the channel. The main characteristic of the receiving station is the radius of the receiving telescope **rx\_aperture**, that determines the quantity of light that cannot be collected by the receiver. The beam wandering effects are characterized by the index-of-refraction structure constant **Cn2** and, in the satellite-to-ground case, also by the pointing error **sigmaPoint**. The model assumes a constant Cn2 through the whole propagation [2]. The last parameter is the atmospheric transmittance **Tatm**, that takes into account the attenuation due to atmospheric absorption.

The model assumes that each qubit is affected by the PDTC independently from the other qubits of the transmission. Despite being highly unrealistic, since it neglects the dynamics of the atmosphere, that is way slower than the typical time difference between two

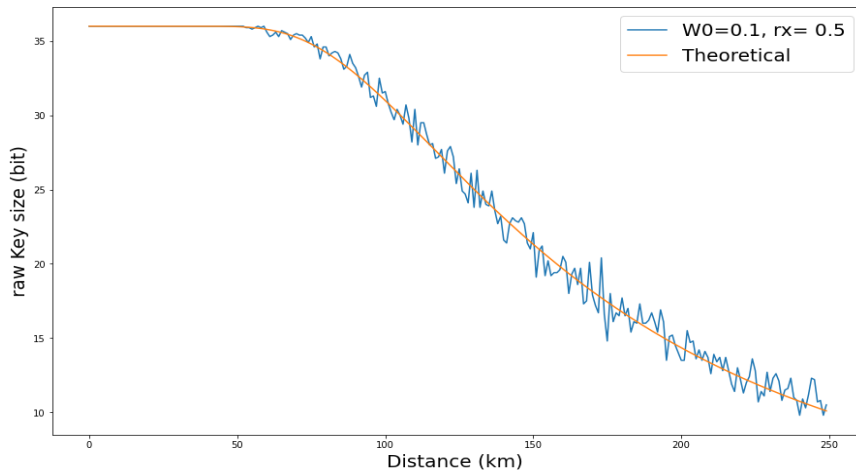
qubits, it allows to provide a good insight of the average properties of the channel. In addition to this, the satellite-to-ground channel assumes a fixed position for the satellite. This allows to give a first estimate of the performance of the channel when the satellite is on a given position in the sky, but it lacks the ability to provide information about a long-time operation on the channel, which requires to calculate externally the different positions of the satellite with respect to time and to make a separate simulation for each of them. Future implementations of the model will address this issue.

### 4.2.2 Verifying correctness of the simulation code

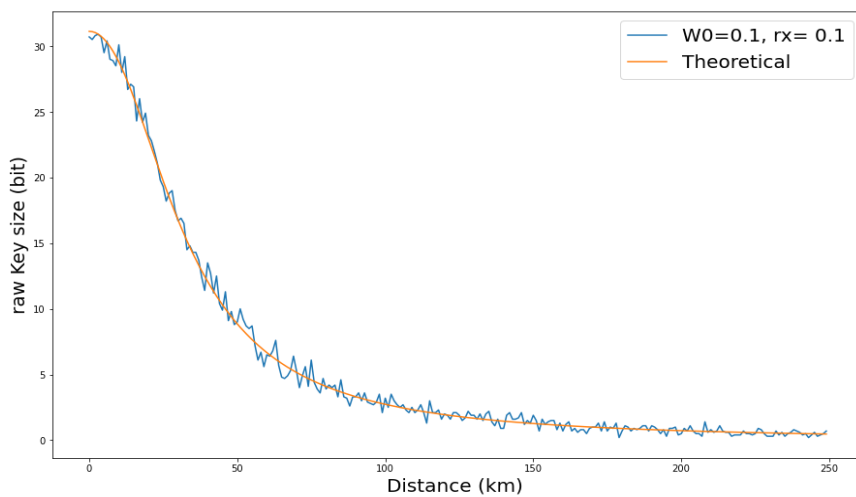
As a first validation of the model, we simulate the transmission of a qubit from Alice to Bob through free space. The simulation runs for 75 ns and we simply count the number of clicks at the receiver end (raw key size). Every operation is supposed to be perfect (creation of qubit, measurement) except for the passage through the free space channel. Every operation takes one nanosecond to perform. We simulate the number of qubits arriving at Bob's detector for different values of  $W_0$  and  $r_x$  (in m), in the case of  $C_n=0$ , and compare it to the theoretical curve, corresponding to the simple diffraction losses of the Gaussian beam on a fixed radius aperture. The wavelength is fixed at 1550 nm for all simulations. We observe good agreement between our implementation and the theoretical model, indicating the correctness of our code implementation.



Comparison of simulated and theoretical ground-to-ground free-space channel transmittance with simple diffraction losses (atmospheric coherence length  $C_n=0$ ) at 1550 nm.



Comparison of simulated and theoretical ground-to-ground free space channel without atmosphere ( $C_n2 = 0$ ) at 1550 nm.



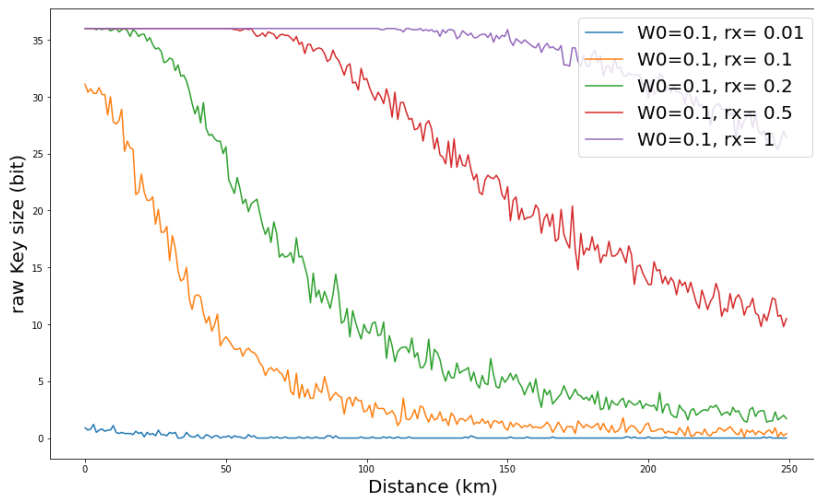
Simulation of free-space ground-to-ground channel with same size transmitting and receiving telescopes, without atmosphere ( $C_n2 = 0$ ) at 1550 nm.

### 4.2.3 Parameter study

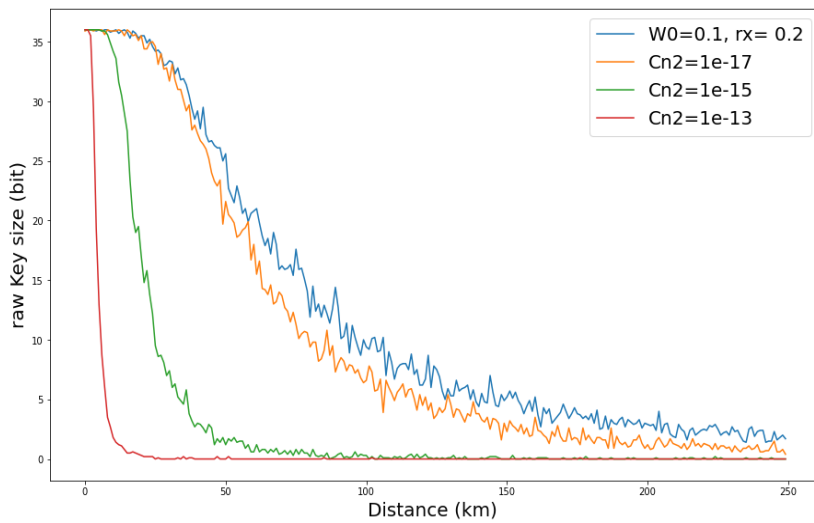
Here we investigate the relative influence of the various parameters of our free-space channel model on the rate at which raw key can be generated.

#### Free-space channel

First, we consider a free-space channel between two ground stations Alice and Bob. Alice perfectly creates and sends photonic qubits in one of the BB84 states [5] every 1 ns to Bob. We count the number of clicks at Bob's detector, considering perfect measurements. We run this simulation for 7 5ns. We separately vary the aperture of the receiving telescope (varying  $rx$ , while we keep  $C_n2=0$ ) and the effect of the refraction index of the atmosphere (varying  $C_n2$ , while we keep  $rx = 0.2$ ) and plot the results below. We observe that increasing  $C_n2$  leads to a greater decrease in the amount of key obtained than a decrease of  $rx$ .



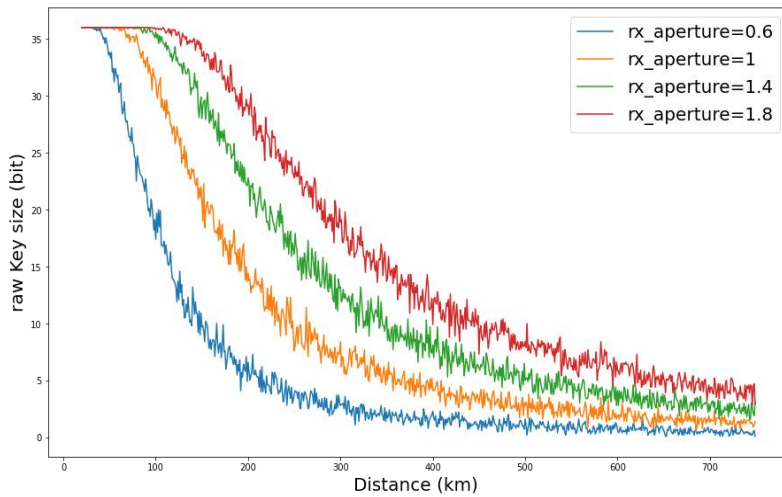
Simulation of the ground-to-ground free-space channel transmittance without atmospheric turbulence ( $Cn2 = 0$ ) for different sizes of the receiving telescope.



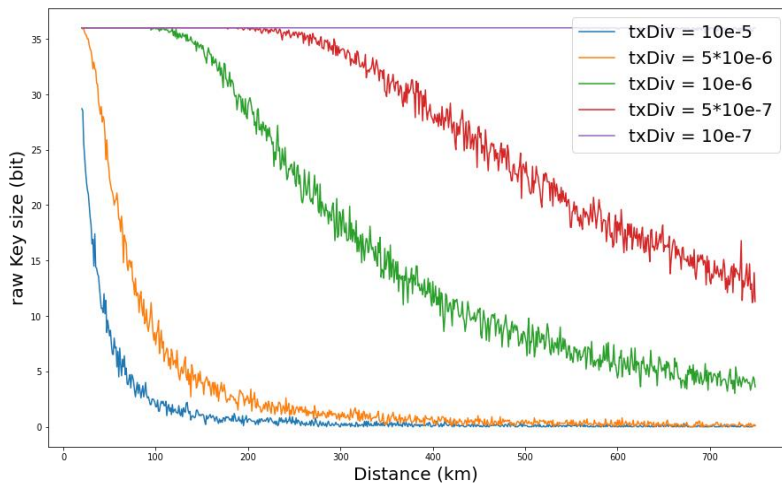
Simulation of the free-space ground-to-ground channel for different values of turbulence strength.

**Satellite to ground channel**

Next, we consider the channel for satellite-to-ground transmission of photons. The satellite creates photonic BB84 states every 1 ns and sends them to a ground station Alice. We run the simulation for 75 ns and we count the number of clicks at Alice’s detectors. We first vary the radius of the receiving telescope ( $r_x$ , while other parameters are set at  $TxDiv=10e-6$ ,  $\sigma_{point}=0.5e-6$ ,  $Cn2=0$  and  $T_{atm} = 1$ ), followed by varying the divergence of the beam sent from the satellite, corresponding to a transmitting telescope radius ranging from 3 mm to about 30 cm (the other parameters are set at  $\sigma_{point}=0.5e-6$ ,  $r_{x\_aperture} = 1.8$ ,  $Cn2=0$  and  $T_{atm}=1$ ). We plot the results below. We observe that enlarging the radius of the receiving telescope has a larger influence on the raw key distribution rate than making the beam divergence smaller.



Simulation of the satellite-to-ground channel for different sizes of the receiving telescope. The effects of atmospheric turbulence are considered negligible with respect to the pointing error.



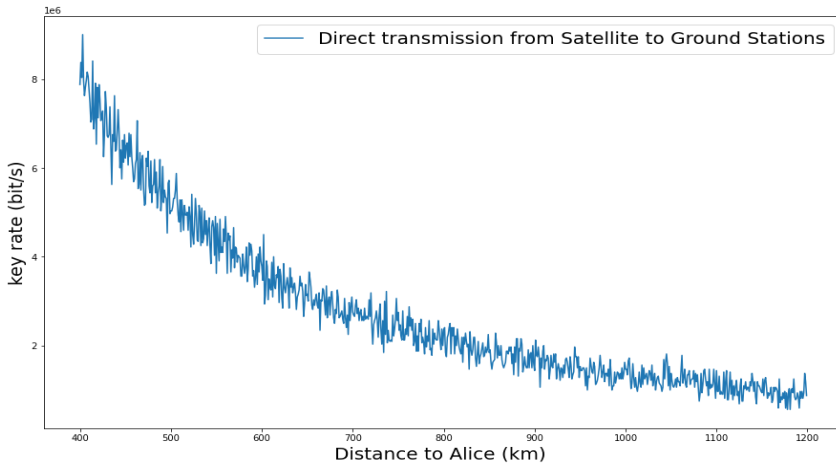
Simulation of the satellite-to-ground channel for different values of divergence for the transmitter beam, considering a receiving telescope of radius 1.8 m and neglecting atmospheric turbulence.

These simulations help us investigate the theoretical possibilities of free space links and satellite to ground links.

#### 4.2.4 Application to a simplified real-world scenario

Here, we obtain the rate at which key can be distributed at realistic parameters ( $\text{txDiv} = 5\text{e-}6$ ,  $\text{sigmaPoint} = 0.5\text{e-}6$ ,  $\text{rx\_aperture} = 0.6$ ,  $\text{Cn2} = 0$  and  $\text{Tatm} = 1$ ).

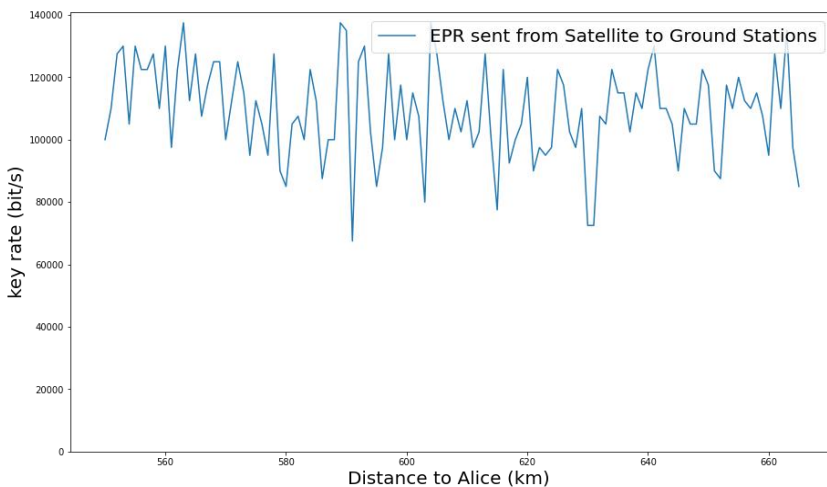
We first study the transmission between a single satellite and a single ground station (called 'Alice'). We suppose that the creation of each BB84 state at the satellite is perfect and takes 1 ns and the same for measurements at the ground station. We show the raw key rate as a function of the distance from the satellite to Alice.



Raw key rate for a quantum transmission from a satellite placed at the mid-point between Paris and Delft, at an altitude of 550 km, and the ground station in Paris (with a telescope of 60 cm radius).

In the second setup, there are two ground stations: one in Paris and one in Delft (377 km distance), and a single satellite at 550 km altitude in between Alice and Bob. In a single round of the protocol we simulate, the satellite produces an EPR pair and sends one qubit of the pair to Alice and the other to Bob. Following the Ekert91 [6] protocol, Alice and Bob measure their qubit in a randomly chosen basis. We only store the measurement outcomes where Alice and Bob measured in the same basis.

We simulate the protocol above for varying distances between Alice and the satellite. For each distance, we perform four runs of the protocol, each lasting 10000 ns. For each distance, we plot the average raw key rate over the four runs. The parameters are  $txDiv = 10e-6$ ,  $sigmaPoint=0.5e-6$ ,  $rx\_aperture=1$ ,  $Cn2=0$  and  $Tatm=0.9$ ; the EPR pair is perfect and its generation takes 2 ns (so the source emits at a rate of 500 Mpairs/s), measurements at the ground stations are perfect. We find that the raw key rate is on the order of 100 kbit/sec. The loss induced by the growing distance between the satellite and Alice is compensated by the shortening distance between the satellite and Bob.



Sifted key rate for entanglement-based QKD between Paris (Alice) and Delft (Bob) exploiting a satellite placed at a 550 km altitude between the two cities. The two ground stations have a 1 m radius receiving telescope.

## 4.3 Conclusion

In this part of the deliverable, we have described the implementation of a model for photon transmission through a free-space channel to be used as a building block for a NetSquid computer simulation of a quantum network. We have used it to investigate the implementation of quantum key distribution using a single satellite node, with the simplifying assumption of no imperfections in the quantum operations at the nodes.

First, we studied the influence of several parameters of the model on the rate at which key can be distributed, and found that the key rate is most influenced by the refraction index of the atmosphere, indicating that weather conditions are an important factor to take into account in future assessment studies. A less influential parameter is the aperture of the receiving telescope, while the divergence of the beam has an even smaller effect.

Next, we simulated quantum key distribution through a single satellite using realistic parameters between Paris and Delft, and with a photon emission rate of 500 MHz, obtained key rates of 100 kbit per second.

## 4.4 References

[1] <https://github.com/matteoschiav/netsquid-freespace>

[2] D. Yu. Vasylyev, A. A. Semenov, and W. Vogel, *Toward Global Quantum Communication: Beam Wandering Preserves Nonclassicality*, Phys. Rev. Lett 108, 220501 (2012)

[3] D. Dequal, L. Trigo Vidarte, V. Roman Rodriguez et al., *Feasibility of satellite-to-ground continuous-variable quantum key distribution*, npj Quantum Inf 7, 3 (2021)

[4] D. Vasylyev, W. Vogel, and F. Moll, *Satellite-mediated quantum atmospheric links*, Phys. Rev. A 99, 053830 (2019)

[5] Bennett, Charles H., and Gilles Brassard. "Quantum cryptography: Public key distribution and coin tossing." *arXiv preprint arXiv:2003.06557* (2020).

[6] Ekert, Artur K. "Quantum cryptography based on Bell's theorem." *Physical review letters* 67.6 (1991): 661.

## 5. Part 2: Satellite-based communication with quantum memories

### 5.1 Introduction

Distributing quantum information over long distances is one of the main challenges of quantum communication. For short distances optical fibers provides an excellent solution and has enable both technological breakthroughs such as quantum cryptography and advances in fundamental science, e.g. loophole free violation of Bell's inequality. For longer distances loss of photons from optical fibers limits the achievable distance to a few hundred kilometers. Within QIA we are intensively investigating quantum repeaters as a means to overcome this limitation. The fundamental idea is to probabilistically generate quantum entanglement over short distances heralded by a measurement outcome and store the generated entanglement in a quantum memory. The entanglement generated in one segment of the channel can then later be merged with entanglement generated in another segment through entanglement swapping thereby extending the distance. Since entanglement generated in one segment can be stored in the quantum memory until the second succeeds, this procedure changes the scaling with distances from exponential to polynomial, thus putting long distance quantum communication within reach.

The longest quantum communication ever achieved has been achieved with a source of entangled photons placed on a satellite. Since photons can travel freely through empty space, this has enabled the distribution of entanglement to receivers separated by a ground distance  $L_g = 1200\text{km}$  [Yin17]. The probability to detect a single photon from a satellite  $p_d$  is however very limited, e.g.  $p_d \lesssim 10^{-3}$  for the low earth orbit satellite of [Yin17]. Since the pair probability scales quadratically with the downlink probability  $p_d^2$ , this severely limits the achievable communication speed. This problem is greatly enhanced if we consider satellites in higher orbits to allow for a longer duration of the line-of-sight between the receivers and the satellite. From diffraction of optical beams one expects that the probability scales as  $p_d \sim L^{-2}$ , where  $L$  is the height of the satellite. Extending the current orbit height of  $L = 500\text{ km}$  to geostationary orbit of  $L \approx 36.000\text{ km}$ , would thus have a scaling of  $L^{-4}$  resulting in a reduction of communication speed by a factor of  $\sim 2 \cdot 10^7$ .

To increase the speed of quantum communication and extend it to even longer distances it has been proposed to combine satellite based quantum communication with quantum repeater technologies to exploit the advantages of each of the approaches [Bon15,Gün20]. We have theoretically explored an approach similar to Ref. [Gün20] and investigated the use of quantum memories on satellites. By placing quantum memories on the satellite, entanglement can be generated between a ground receiver and the satellite with rate proportional to  $p_d$ . Establishing an entanglement link between the satellite and a second receiver and performing entanglement swapping then enable communication between the two receivers. Since both entanglement generations occur with a rate proportional to  $p_d$ , the rate of the protocol only scales linearly with  $p_d$  and can potentially be much faster than the direct transmission of pairs.

While the use of quantum memories can potentially improve the rate of communication with satellites, numerous practical considerations limit the advantage of this approach. Most notably quantum memories have limited storage time and the available number of quantum memories is limited. The entanglement swapping on the satellite needs to be conditioned on a successful

heralding of the entanglement generation, and the heralding signal may have to travel from the ground receiver to the satellite. This puts stringent requirements on the quantum memories. Furthermore, current quantum memories typically have a smaller bandwidth than the repetition rate of the photon-down conversion setups used in current satellite experiments [Yin17]. This further challenges the advantage of the memory based approach.

We have theoretically explored a number of different physical setups similar to the setups being developed within QIA. We have estimated their potential for memory enhanced quantum communication with satellites and determine the memory requirements for improving the communication rate. A similar analysis was presented for a single setup in [Gün20], but we have made a much broader investigation, including several scenarios not included in that work. We calculate the achievable communication rate given realistic values for the efficiency and decoherence rates of the memories. In practice numerous other imperfections, such as gate errors, may also affect the quantum communication. The full inclusion of such effects is beyond the scope of this work and we focus on the imperfections imposed by the quantum memories. The full details of the investigation is presented in [And20]. Here we will not go into the full detail but only provide a summary of the main results.

Below we first review the main physical systems that we have considered and then move on to discuss various setups for memory enhanced communication. We consider two different scenarios. First, we consider a situation similar to quantum key distribution (QKD) where the receivers immediately measure the photons they receive in some basis. Secondly, we consider more advanced applications where the receivers want to store entanglement at the ground stations for further applications, e.g. for the generation of a repeater link [Bon15] or a full-scale quantum internet.

## 5.2 Physical systems considered

In this section we briefly review the main physical systems that we consider and discuss the properties that will be important here.

### 5.2.1 Satellite Link

The most central quantities in the connection between receivers and satellites are the efficiency and quality of the link. For the experimental configuration in Ref. [Yin17] polarisation encoding of quantum information was used and to a high degree preserved the quantum state during transmission. It is likely that a similar performance can also be obtained using time bin encodings. Here we will therefore only focus on the efficiency of the link and neglect any degradation of the quality as well as any dark counts at the detectors from stray light.

The efficiency of transferring a photon between a satellite and a ground station depends on a number of parameters including the size of the telescopes used, the distance to the satellite, atmospheric absorption at the wavelength used and the amount of turbulence [Bou14]. Numerous estimates for the attainable value exist. For a downlink experiment where photons are sent from a satellite to the ground we will assume a value similar to Ref. [Yin17] and take the probability to successfully detect a photon to be  $p_d = 10^{-3}$  for a satellite in a low earth orbit with a receiver to satellite distance of  $L = 1000$  km. Uplink experiments, where photons are sent from the ground to a satellite are more susceptible to atmospheric noise. In Ref. [Ren17] such an uplink experiment was performed with a peak transmission probability near  $p_u = 10^{-4}$  for a similar distance. We will therefore use this value for our numerical estimates. We emphasise, however, that these numbers depend heavily on the specific implementations as well as the time varying angle of the

line of sight during the passage of the satellite. The numbers we derive here are only intended to provide rough guidelines to what can be achieved. For all of the protocols we consider we will derive the scaling with the link efficiencies to allow an easy comparison to other parameters.

For protocols which rely on a heralding signal another important factor is the communication time between the ground and the satellite  $T_{com}^{s \leftrightarrow g} = L/c$  or in some cases the communication time between the two ground stations  $T_{com}^{g \leftrightarrow g} = L_g/c$ . These quantities will be important for assessing the memory requirements below.

## 5.2.2. Photon sources

Current experiments with quantum communication to satellites [Yin17, Ren17] use spontaneous parametric down-conversion (SPDC) as a source of entangled photons. In this process a photon is converted into two photons in an entangled state with a low generation probability  $p_s \ll 1$  thereby generating a quantum state of the form

$$|\Phi\rangle = |\emptyset\rangle + \sqrt{p_s} \psi^{-} + O(p_s),$$

where  $\psi^{-} = (|01\rangle - |10\rangle)/\sqrt{2}$  is the desired maximally entangled state of two photons with two different logical states  $|0\rangle$  and  $|1\rangle$ , e.g. two polarisation or time-bin states, and  $|\emptyset\rangle$  denotes the vacuum state. The last term denotes events with more than one SPDC event and introduces an error in the conditional fidelity of all states with a probability proportional to  $p_s$ . For most of our estimates we will take a rather low value  $p_s \sim 10^{-2}$ . Some of the protocols considered will involve more than one SPDC source and in this case we take into account that the error rate increases since now erroneous events can happen in each of the sources.

The fact that SPDCs have to be run with a very low generation probability  $p_s \ll 1$  provides a large reduction of the communication rate. To overcome this it would be desirable to have access to deterministic sources of entangled photons. Although much progress has been achieved, such sources are not readily available at the moment. Nevertheless, we can estimate the achievable rates with such sources by simply setting  $p_s \approx 1$  and ignoring the associated reduction in fidelity.

A major advantage of most photon sources is that they can be operated at very high speed. In our estimates we will assume that they operate with a repetition rate up to  $r_{rep} = 10^8$  Hz [Yin17, Ren17]. Quantum memories on the other hand often cannot run at such a high bandwidth and this has to be taken into account for assessing the advantage of exploiting quantum memories. Furthermore protocols conditioned on the arrival of a heralding signal will typically have to be run at a slower rate since they depend on the communication time to the satellite  $T_{com}^{s \leftrightarrow g}$ . We will include these considerations in all of the considered protocols.

## 5.2.3 Quantum emitters

In QIA we are heavily investigating quantum emitters within WP1. Here we will explore how these might be employed to boost the communication rate of satellite communication. A method to realise heralded entanglement between distant quantum memories is to have a single quantum emitter, which emits single photons entangled with the internal state of the emitter. Performing entanglement swapping between photons from two such emitters generates entanglement between the two emitters. Such protocols have been realised in a number of different system and is major area of research within QIA. Generally the protocols for this can be divided into single-photon and two-photon protocols, depending on how many photons are detected in the entanglement swapping.

The single-photon protocols are typically advantageous if the entanglement swapping takes place halfway between the emitters in which case it leads to a higher entangling rate. Single photon protocols are, however, often harder to implement since they require the optical path length to be stabilised to within an optical wavelength. Given that it will be hard both to stabilise the path length of a satellite link and to perform entanglement swapping halfway between the ground and the satellite, we will focus on two-photon protocols.

In the two-photon protocols each emitter sends out a quantum state of the form  $\Psi^{-}$  but now with  $0\rangle$  and  $1\rangle$  for one of the two subsystems referring to the internal state of the emitter. Impinging the photons from two emitters on a suitable combination of beam splitters and conditioning on a specific output then implements a Bell state measurement on the photons, which projects the two emitters into a maximally entangled state e.g.  $\Psi^{-}$ . If implemented with linear optics such a Bell state measurement has a swapping efficiency of at most  $\eta_{swap} = 0.5$ . In addition to this, emitters have a finite collection efficiency  $\eta_c < 1$ , which further reduce the probability of detecting the photons. Much effort has been put into improving this efficiency and recently a combined collection and detection efficiency of  $\eta_c = 85\%$  was reached for SiV center in diamond [Bha20]. We will therefore assume rather high values of the efficiency in our estimates  $\eta_c \gtrsim 0.5$ .

One of the main challenges of all quantum memories is that the stored information decay with time. For qubits stored in the internal degrees of a single quantum emitter, the fidelity of the stored state will typically decay exponentially in time with a characteristic decay constant  $\tau_\eta$ . The memory time depends heavily on the system used, but experiments have e.g. reached memory times of up to  $\tau_\eta = 75$  s for NV centers in diamond [Bra19] whereas trapped ions have achieved even longer times  $\tau_\eta > 10$  minutes [Wan17]. Combining such long memory times with all the other ingredients required for the protocols will be challenging and the memory coherence times will thus be one of the most critical parameters we investigate. Another issue to consider is the nature of the decay, i.e. which state the qubit decays into. For simplicity we will consider a worst case model and assume that the qubit approaches a completely mixed state. This means that any memory decoherence will directly affect the quality of the stored state and has to be kept very small.

Compared to single photon sources a drawback of quantum emitters is that they typically have a smaller bandwidth. This means that they have to be operated at lower repetition rate. In most cases however, the repetition rate will be limited by the communication time  $T_{com}^{S \leftrightarrow G}$ , so that this is not the main limitation. For some of the protocols, however, it will matter. In those cases we will assume a maximum repetition rate  $r_{rep} = 3 \cdot 10^7$  Hz slightly enhanced compared to Ref. [Bha20], which have conditions similar to what we explore, where mapping to the memory can be attempted several times, without resetting the emitter.

An essential ingredient in the memory enhanced protocols is entanglement swapping between qubits stored in the quantum emitters. If multiple qubits are stored in different internal states within the same emitter, e.g. different nuclear spins in NV centers in diamond, such entanglement swapping can be achieved by simply exploiting the coupling within the emitter. A drawback of this is that a second entanglement attempt with the same emitter may influence the quality of the stored state. This is e.g. an issue for NV centers [Kal17]. In that case an alternative is to map the state of the emitters onto photons and perform optical Bell state measurements, although this will reduce the efficiency by a factor of  $\sim \eta_c^2 \eta_{swap} < 0.5$  due to the limited collection and swap efficiency (this could be remedied by using more advanced Bell state measurements [Wit12]). On the other hand this approach allows multiplexing a large number of quantum memories  $N_{mem} \gg 1$ , which reduce the requirements for the memory coherence time by a factor of  $N_{mem}$  [Col07].

## 5.2.4 Ensemble based memories

Another class of quantum memories investigated in QIA within WP2 is based on ensembles of emitters. In these systems light is not stored in a single emitter but rather in a collection of them. A particular attractive feature of these systems is that they are fairly simple systems, which naturally allow for simultaneous storage of multiple modes  $N_{mem} \gg 1$ . Currently up to  $N_{mem} = 225$  optical modes have been stored simultaneously [Pu17].

A drawback of the ensemble based approach is that the systems do not easily allow for gates between stored qubits. Entanglement swapping thus has to be rely on reading out excitations optically and performing optical Bell state measurements. This limits the efficiency to  $\eta_{swap} \leq 50\%$  achievable with linear optics.

For the protocols we explore ensemble based quantum memories will only be used for storage of photons generated by SPDC. We will therefore assume that they can be characterised by only two numbers, the efficiency of retrieving a stored photon  $\mu$  and the memory coherence time  $\tau_{\mu}$ . An attractive feature of the ensemble based memories is that in practise memory decoherence predominately leads to loss of efficiency and not degradation of the quality of the state if a photon is detected. We will thus model memory decoherence as an exponential decay of the efficiency from its initial value with no degradation of the state conditioned on the detection of a photon. This particular decoherence mechanism is advantageous because it allows extracting information stored in the memory for times comparable to the decoherence time. In this case there is a sizeable probability that the photon is lost, but if we are only concerned with the state conditioned on the detection of a photon, this is a minor concern. This is in contract to protocols based on quantum emitters, where the fidelity decays with time. Below we often find similar inequalities describing the requirements for the memory coherence time for emitters and ensembles, but these inequalities are much more stringent for the emitters, where the inequalities have to be satisfied by a much larger factor.

## 5.2.5 Photon scattering gates

We have found that a highly desirable building block for the memory enhanced communication that we explore in the present work, is a gate operation between an incoming photon and a stationary qubit. Within QIA such gates are being explored by the group at MPQ. In these gates an incoming photon scatters off a cavity, strongly coupled to a transition from an internal level  $|1\rangle$  to some excited state, whereas another internal level  $|0\rangle$  is not coupled to the cavity field. Ideally this will result in a transformation

$$|0\rangle \rightarrow \nu |0\rangle$$

$$|1\rangle \rightarrow -|1\rangle$$

if a photon is incident on the cavity, whereas nothing happens if no photon is incident. This dynamics is particularly useful because it e.g. allows a quantum non-demolition measurement of the presence or absence of a photon: Suppose that an atom is initially prepared in a superposition  $(|0\rangle + |1\rangle)/\sqrt{2}$ . The scattering of an incident photon will thus change the atomic state into an orthogonal state  $(|0\rangle - |1\rangle)/\sqrt{2}$  allowing the determination of whether a photon was incident. This is useful because it for instance allows us to restrict the number of memories to those where a photon actually made it from the satellite to the receiver. Furthermore the dynamics described here can also be used to map the state of an incoming photon onto the stationary qubit conditioned on the detection of the photon. This will be a very useful resource for the protocols we consider below.

## 5.3 Applications for QKD

As a first example we consider a scenario where two communicating parties, Alice and Bob, are interested in performing quantum key distribution (QKD). This application is particularly simple since Alice and Bob can immediately measure their respective qubits in a suitable basis. There is thus no need for them to have quantum memories and the only memories we consider are on the satellite.

A summary of the results we obtain are presented in Table 1. Here we give expressions for the communication rate as a function of the parameters of the setup. The rate is given in the good memory regime, where the memory coherence time is sufficiently long to allow for a rate scaling linearly with the relevant up- or down-link probability  $p_u$  or  $p_d$ . The requirements on the memory time to achieve this limit is indicated by  $\tau$ . Furthermore we give example parameters to achieve a communication rate of  $R = 1$  Hz comparable to what can be achieved with a direct downlink with the same parameters. Improving the parameters beyond these numbers allow for a faster communication time using the memory based approach. Finally we give the scaling with the height of the satellite  $L$ , assuming that losses are diffraction limited so that the up- or down-link probability scales as  $L^{-2}$  and the communication times scales as  $L$ . As it is clear from the table, various memory based solutions allow for outperforming the direct approach provided a sufficiently high number of memories and long coherence time can be achieved. Below we go into more details with each of the schemes considered in the table.

From the numbers in table 1 it is clear that it is challenging to reach a performance comparable to the direct downlink. We note however, that it is hard to improve the numbers for the direct downlink, except perhaps by creating deterministic sources of entangled photons, which would also improve some of the other protocols. This means that it will be hard to significantly improve the parameters of that method. The numbers listed for the memory based approaches are those required to reach the benchmark of  $R = 1$  Hz and thereby break even with the direct approach. If we can improve the memory parameters beyond those values, the memory based approaches are advantageous. Furthermore all of the memory based approaches have a better scaling with the satellite height. This means that they become more advantageous for higher satellite heights.

Scheme	Rate	$\tau$	Benchmark		$L$ -scaling
			$N_{mem}$	$\tau$	
Direct downlink	$p_d^2 p_s r_{rep}$	-	-	-	$L^{-4}$
Ensemble downlink	$\frac{1}{3} \mu^2 N_{mem} p_s p_d / T_{com}^{S \leftrightarrow G}$	$\tau_\mu \gg \frac{T_{com}^{S \leftrightarrow G}}{N_{mem} p_s p_d}$	1000	0.5 s	$L^{-3}$
Emitter downlink	$\frac{2}{3} \eta_{swap} N_{mem} p_d \eta_c \frac{1}{T_{com}^{S \leftrightarrow G}}$	$\tau_\eta \gg \frac{T_{com}^{S \leftrightarrow G}}{\eta_c p_d}$	15	60 s	$L^{-3}$
Emitter uplink	$\frac{2}{3} \eta_{swap} p_s p_u \eta_h r_{rep}$	$\tau_\eta \gg \frac{1}{p_s p_u \eta_h r_{rep}}$	1	0.2 s	$L^{-2}$

Table 1: Overview of considered options for QKD with memories on satellites. The Rate column express the estimated rate in the regime, where the memory coherence time fulfil the requirement listed in the column  $\tau$ . Benchmark describes example parameters for the number of memories  $N_{mem}$  and coherence time  $\tau$  allowing a rate of  $R = 1$  Hz , comparable to what has been achieved with direct downlink for a satellite height  $L = 1000$  km.  $L$ -scaling describe the scaling with satellite height assuming that the losses are mainly limited by diffraction. For the emitter downlink the memory coherence time can be reduced by a factor of  $N_{mem}$  by multiplexing the quantum memories. For the emitter uplink the benchmark numbers don't fully satisfy the listed memory requirements, and this is taken into account in the calculated rate. The rate can in this case be improved by improving the memory time. See detailed discussion for assumptions going into these numbers.

### 5.3.1 Direct downlink

The direct downlink represents the setup implemented in current satellite experiments. It consists of a SPDC source emitting pairs of photons, which are detected at two ground receivers. To keep the number of emissions of double-pairs to a minimum, the source must be operated with a low source efficiency  $p_s \ll 1$  There is no memory required for this protocol, which means that it can be operated at a very high repetition rate  $r_{rep}$ , only limited by technological limitations of how fast the source and detectors can be made. This leads to a communication rate  $R = p_d^2 p_s r_{rep}$ . For the satellite experiments we have  $p_s r_{rep} = 5.9 \cdot 10^6$  Hz. With  $p_d = 10^{-3}$  this leads to a communication rate of  $R = 6$  Hz, in rough agreement with the measured results, with the difference being due to choosing a rounded value for  $p_d$ . For these parameters the satellite experiments reach a fidelity around  $F \gtrsim 90\%$ .

This example will serve as a benchmark for the performance of the protocols considered below, where we seek parameters to allow for a similar performance. To allow for further reductions in the Fidelity due to technical imperfections, we therefore aim to achieve a fidelity  $F \geq 95\%$  when considering concrete parameters.

### 5.3.2 Ensemble downlink

The ensemble downlink approach is based on having two SPDC sources on the satellite. One of the outputs from each source is sent to the ground, while the other is sent to a multimode memory. The satellite keeps sending out photons until the memory is full.

A memory mode is then erased if the receiver reports back that no photon was detected or kept and used for entanglement swapping if the receiver detected the photons.

The main obstacle for this protocol is the relatively long communication time between ground and satellite  $T_{com}^{S \leftrightarrow G}$ . To have any advantage of the memory, the memory coherence time  $\tau_\mu$  must exceed this communication time  $\tau_\mu \gtrsim T_{com}^{S \leftrightarrow G}$ . A more stringent requirement, however, comes from the fact that the entanglement generation time is much longer the communication time  $T_{com}^{S \leftrightarrow G}$ . With  $p_d = 10^{-3}$  and source probability in the range  $p_s = 10^{-2} - 10^{-1}$  it requires  $N_{mem} = 10^4 - 10^5$  to have a sizeable probability to generate entanglement within a communication time  $T_{com}^{S \leftrightarrow G}$ . For smaller numbers of memories a generated entanglement in one memory must survive for a time  $\tau_\mu \gg \frac{T_{com}^{S \leftrightarrow G}}{N_{mem} p_s p_d}$  to enable swapping when a second photon is detected in the other arm. If the swapping then succeeds with a probability  $\eta_{swap}$  we arrive at a communication rate  $R = \frac{1}{3} \mu^2 N_{mem} p_s p_d / T_{com}^{S \leftrightarrow G}$ , where  $\mu$  is the memory efficiency and the factor in front is a combination of 50% swap probability and a factor of 2/3 between the average rate of creating single successful events and pairs of them.

As a particular example we find that parameters of  $N_{mem} = 1000$ ,  $\mu = 0.9$ , and  $\tau_\mu \gtrsim 0.5$  s allows for a generation rate  $R = 1$  Hz with a Fidelity  $F = 0.95$ .

### 5.3.3 Emitter downlink

One of the major drawbacks of the ensemble based approach considered above is the need for a very low source probability  $p_s \ll 1$  in order to maintain a high fidelity. This affects not only the rate but also the required number of memories and coherence time. A possible solution could be to replace the SPDC source and ensemble based memory by a single quantum emitter. This will allow increasing the source efficiency to  $p_s = \eta_c$ , where  $\eta_c$  is the collection efficiency of the emitter, without any detrimental effect on the fidelity. We can thus describe this situation by inserting  $p_s = \eta_c$  in the result above with some minor modifications discussed below.

For the entanglement swapping there are now various options for how to proceed. Either one can exploit that after entanglement generation, the quantum emitter may possess some kind of built in quantum memory, which allows storage of the entanglement while another entanglement generation is being attempted. This is for instance the case for NV centers, where entanglement is generated with the electron spin. The electron spin can be decoupled from the nuclear spin, which can act as a quantum memory. In this case one perform entanglement swapping with unit efficiency  $\eta_{swap} = 1$  by using the internal dynamics of the NV center. In this scenario, however, one cannot reduce the memory time requirement by having several memories in parallel. Multiple memories thus only increase the total rate by allowing parallel operation. The requirements for the memory coherence time are further enhanced by the fact that decoherence reduce the fidelity not the efficiency, thereby putting more stringent requirements on the inequality for the memory coherence time (the inequality should be fulfilled by a larger factor).

In practice there will typically be some degradation of stored entanglement, while another entanglement is being generated. Therefore it may be an advantage to instead employ completely independent emitters. In this case the entanglement swapping can, e.g., be achieved by mapping an excitation onto light and performing linear optics Bell state measurement with an efficiency  $\eta_{swap} = \frac{1}{2}$ . Simultaneously this would also reduce the required memory coherence time by a factor of  $N_{mem}$  [Col07].

Which of the two swapping approaches considered above that is advantageous depends on the details of the practical implementation. Here we consider the first approach and find that we can reach the benchmark of  $R = 1\text{Hz}$  and  $F = 0.95$  with  $N_{mem} = 15$ ,  $\tau_\eta = 60\text{s}$  and  $\eta_c = \eta_{swap} = 1$ .

### 5.3.4 Emitter uplink

The main limitation for the setups considered above is the communication time between the ground and the satellite. This means that relatively long time is spent waiting for a signal to arrive at the satellite with information about whether the photon was detected at the ground station. This problem can be overcome using a protocol where photons are sent from the ground to the satellite. The arrival of a photon at the satellite and storage into a quantum memory is heralded by a click in a detector as described below. One memory node is communicating with each of the two ground stations. Once both memories have successfully registered a photon, the entanglement can be swapped and the parties on the ground are informed which entanglement attempts succeeded.

In this scheme the heralding is done at the satellite, which also performs the entanglement swapping. Hence there is a very short communication time, since it only has to be communicated within the satellite. This means that the protocol can be run at a very high repetition rate  $r_{rep}$ , which significantly increases the final communication rate. On the other hand, since the protocol is based on uplink, we have to take into account that the uplink probability  $p_u$  is typically much smaller than the downlink probability and we take  $p_u = 10^{-4}$  for concrete numbers.

For the heralded storage into the quantum memories we have considered two options. One is based on having an emitted emit a photon entangled with its internal state. Mixing this photon with the signal from the ground and conditioning on the detection of two photons, teleports the state of the photon into the quantum memory. The drawback of this method, however, is that the signal from the ground is very weak. This means that if two photons are emitted from the emitter there is a large probability that the detected signal will be dominated by this noise. This puts very stringent requirements on the emitter. Instead we consider photon scattering gates, where the incoming photon scatters off the emitter and transfers its state to the emitter with some heralding probability  $\eta_n$ . Since there is no other light at the emitter during the scattering, the detection of a photon will be dominated by the photons arriving from the ground provided that there is a limited number of dark counts. We believe that this will make the protocol more robust to imperfections.

A major advantage of this protocol is that it put very limited demands on the quantum memories. Because the storage is heralded and the heralding station is right next to the memory, we can immediately erase unsuccessful attempts. This also implies that there is little gain by having multiple memories on the satellite and the entire protocol can be run with  $N_{mem} = 1$ .

For the entanglement swapping there are again similar consideration for how to perform the entanglement swapping as we discussed above. We will for simplicity just assume that it happens with some probability  $\eta_{swap}$ . This protocol further has the advantage that it can be run with coherent states as output of the sources on the ground. This will allow a form of measurement device independent QKD with a source efficiency on the ground approaching unity  $p_s \approx 1$ . A full investigation of this possibility is beyond the scope of this work. To have a better comparison with comparison with other approaches we therefore consider that the sources on the ground are SPDC sources with  $p_s \ll 1$ , where the output in one arm is immediately detected in a detector.

Combining all of these considerations above we arrive at a communication rate  $R = \frac{2}{3} \eta_{\text{swap}} p_s p_u \eta_h r_{\text{rep}}$  provided that the memory time fulfills  $\tau_\eta \gg \frac{1}{p_s p_u \eta_h r_{\text{rep}}}$ . When we insert numbers into these expressions we find that it can outperform most of the protocols considered above. Furthermore, because the protocol is so much faster, we can afford to consider a situation, where we have such a short memory time that we often need to discard the generated entanglement in one arm before the other entanglement succeeds and still reach the desired benchmark of  $R = 1 \text{ Hz}$  and  $F = 0.95$ . Taking a high repetition rate of  $r_{\text{rep}} = 3 \cdot 10^7 \text{ Hz}$ ,  $\eta_h = 1$ ,  $\eta_{\text{swap}} = 1$  and a memory time  $\tau_\eta = 0.2 \text{ s}$ , we find that we can still reach the desired rate  $R = 1 \text{ Hz}$  with a fidelity exceeding  $F = 0.95$ .

## 5.4 Entanglement distribution for application

Above we considered the simplest possible example of quantum communication QKD. For more advanced applications, including a full scale quantum internet as pursued within QIA it is necessary to have the quantum information stored in memories at the ground stations. For this purpose we therefore consider the generation of entanglement between quantum memories at the two ground stations. This situation considerably changes the requirements for the operation of the protocols. Most notably the most efficient protocol above relied on sending multiple photons to the satellite from the ground with a very high repetition rate. When requiring that we have entanglement stored at the ground stations this becomes unfeasible unless we have very large quantum memories at the ground stations. This strongly favours downlink protocols and we will therefore only consider these.

Again we have considered multiple setups that allow for entanglement distribution with or without quantum memories on the satellite. These are summarised in Table 2. For all of the protocols the ability to use the generated entanglement at a later stage requires that we have some kind of knowledge of when the entanglement is available. This necessitates heralding that the photon arrives. For all the schemes we have therefore assumed some kind of heralding based on the photon scattering gates.

From the numbers in the table it is clear that the requirements for beating the direct approach are daunting. Similar to above, however, the direct approach is hard to improve even by employing better memories. Furthermore, the memory assisted schemes are based on a single memory at the ground and can be enhanced by simply having more setups in parallel. This means that the memory based approach may eventually prevail if sufficiently many/good memories are available.

### 5.4.1 Direct downlink

This protocol is the generalisation of the direct downlink protocol employed in current satellite experiments which uses a SPDC source at the satellite. For applications, where entanglement is needed at a later state we need to supplement the protocol with memories at the ground. We consider a scheme where we use the scattering gate to map the state of the photon into a quantum memory. A subsequent detection of the photon heralds the successful storage of the photon in the memory. This heralding is assumed to have an efficiency  $\eta_h$ , which can be of order unity.

Scheme	Rate	Memory time	Benchmark		
			$N_{mem}$	$\tau_\eta$	$\tau_\mu$
Direct downlink	$\eta_h^2 p_d^2 p_s r_{rep}$	$\tau_\eta \gg T_{com}^{g \leftrightarrow g}$	7	1 s	-
Memory assisted, ensemble based	$\frac{1}{3} N_{mem} \mu^2 p_s p_d \eta_h \frac{1}{T_{com}^{s \leftrightarrow g}}$	$\tau_\eta, \tau_\mu \gg \frac{T_{com}^{s \leftrightarrow g}}{p_s p_d \eta_h N_{mem}}$	2000	40 s	4 s
Memory assisted, emitter based	$\frac{1}{3} N_{mem} \eta_c^3 p_d \eta_h \frac{1}{T_{com}^{s \leftrightarrow g}}$	$\tau_\eta, \tau_\mu \gg \frac{T_{com}^{s \leftrightarrow g}}{\eta_c p_d \eta_h N_{mem}}$	20	40 s	40 s

Table 2: Overview of schemes for distribution of entanglement for use in subsequent applications. The column Rate express the rate in the limit where the memory coherence time fulfils the requirement listed in the column memory time. Benchmark: Proposed memory parameters in order to achieve a rate  $R = 0.41$  Hz, as set by the direct downlink scheme.  $\tau_\eta$  refer to the memory coherence time on the ground;  $\tau_\mu$  is on the satellite. These numbers assume a satellite height of  $L = 1000$ km. Note that the number of memories refer to the memories on the ground for the direct downlink. For the memory assisted protocols a single memory is assumed on the ground and the number of memories is on the satellite.

A nice feature of this protocol is that it only needs a limited number of memories. If no photon is detected the memory can be immediately recycled and used for another storage attempt. Once a photon is detected the information has to be stored until one receives a signal from the other receiver about whether that receiver also detected a photon. This time is set by the classical communication time  $T_{com}^{g \leftrightarrow g} = L_g/c$  and this sets the requirement on the memory coherent time  $\tau_\eta$ . Assuming again an optimistic repetition rate of  $r_{rep} = 3 \cdot 10^7$  Hz at the satellite and a source generation probability  $p_s$  sufficiently low to allow for a fidelity  $F \gtrsim 0.95$ , only around 3 photons will arrive at each station within the communication time if the separation between the ground receivers is  $L_g = 1000$ km and  $\eta_h = 0.5$ . This means that only a very limited number of memories is required. In a detailed calculation we find that  $N_{mem} = 7$  is required to achieve a rate of  $R = 0.41$ Hz, close to the maximally achievable rate of  $R = 0.48$ Hz attainable with infinite number of memories. These consideration have been used to defined the input in Table 2, and represents the benchmark that we will try to overcome with memory assisted protocols below.

### 5.4.2 Memory assisted, ensemble based

As first extension of the direct downlink protocol we consider that the SPDC source on the satellite is replaced by two sources and two ensemble based multimode memories. Each SPDC source sends one of its photons to the memory and the other to the receiver on the ground. If the ground receiver informs the satellite that a photon has been detected, the stored photon is used for entanglement swapping once a photon has been detected in the other arm. If no photon is detected on the ground the memory is erased.

The main challenge for this approach is that a very large number of modes needs to be stored at the satellite. Only after receiving a signal from the ground the satellite will know which attempts was successful and therefore all attempts must be kept until that time. At the ground, however, the requirements on the number of memories is much more relaxed since much fewer photon arrives. For simplicity we only consider a single memory on the ground. Thus the numbers we attain here could be boosted by applying several

channels in parallel. By multiplexing these parallel channels such parallel channels would simultaneously lower the requirements on the memory coherence time [Col07].

The main requirement on the coherence time of the memories both at the ground and at the satellite is set by the need for the memories to remain coherent until both entanglement generations has succeeded. This means that the memory coherence time for the memory on the ground  $\tau_\mu$  and on the satellite  $\tau_\eta$  should fulfil  $\tau_\eta, \tau_\mu \gg T_{ent}$ , where the entanglement time is set by  $T_{ent} = \frac{T_{com}^{s \leftrightarrow g}}{p_s p_d \eta_h N_{mem}}$  (assuming that the number of memories is so small that the probability to generate entanglement during each round of the protocol is small). The average time to achieve the entanglement generation is then  $3T_{ent}/2$ , after which the entanglement swapping can succeed with some probability  $\mu^2/2$ , where  $\mu$  is the memory efficiency. This leads to the final communication rate of  $R = \frac{1}{3} N_{mem} \mu^2 p_s p_d \eta_h \frac{1}{T_{com}^{s \leftrightarrow g}}$ . For concrete example parameters we find that we need  $N_{mem} \approx 2000$  memories with  $\tau_\mu \approx 4s$ ,  $\tau_\eta \approx 40s$ ,  $\eta_h = 0.5$  and  $\mu = 0.9$  in order to be comparable to the direct approach with a fidelity  $F \gtrsim 0.95$ . For larger number of memories the memory assisted approach will outperform the direct approach.

### 5.4.3 Memory assisted, emitter based

The main problem with the protocol above is that it assumes a probabilistic source with a low success probability  $p_s \ll 1$ . This means that we have to store a lot of attempts where no photons were emitted. This problem can be directly addressed by replacing the SPDC source and ensemble based memory with a single photon emitter, which deterministically emits photons entangled with the internal state of the emitter. Again we assume that these photons are collected with an efficiency  $\eta_c$ , which can be on the order of unity. In the simplest approach, where we still only consider a single receiver on the ground this leads to a direct reduction in the required number of memories by roughly a factor of 100 for the parameters considered here. With this replacement the number of photons emitted will be the same. Hence the time to generate entanglement will also remain the same. For entanglement swapping, we assume that an approach is used, where the entanglement is generated in two different emitters and then swapped by mapping the excitation to a single photon with the efficiency  $\eta_c$  in order to avoid any detrimental effect on already generated entanglement in subsequent entanglement attempts. These replacements leads to the results for the rate and coherence presented in table 2.

For concrete parameters we take  $\eta_c$  close to unity and arrive at similar parameters as above. The only difference is that now, we need to take into account that memory decay directly affect the fidelity and not just the efficiency. This means that the memory time on the satellite needs to be an order of magnitude larger.

## 5.5 Conclusion

We have explored a number of different approaches for interfacing memory based quantum communication with satellite links. For sufficiently good memories we have shown that such combinations may enhance communication rates compared to what is achievable without memories. Common to all of these approaches is, however, that they puts strong requirements on the quantum memories. The main results have been summarised in Tables 1 and 2. The numbers presented there are challenging but we believe that they are not beyond reach.

The main reason for the strict requirements on the memory parameters is that memory based approaches rely on a heralding signal. For all schemes except the emitter uplink scheme for QKD, this heralding signal has to be sent over long distances. Contrary to the direct approaches, which can be run at a very high repetition rates, this means that most of the time is spent waiting for heralding signals. During this period no photons are sent between the ground and satellite. This immediately points to a path to improving the communication rate: Simply increasing the number of parallel channels, e.g., boosting  $N_{mem}$  by having multiple setups in parallel, directly enhance the communication rate and reduce the requirement on the memory coherence time. Once the quantum memories reach sufficient maturity to allow protocols like the ones considered here, they may thus allow a significant improvement of the communication rate.

## 5.6 References

- [And20] Quantum Key Distribution and Entanglement Distribution with Satellite Links, Anton Lauenborg Andersen, Master Thesis, University of Copenhagen September 2020 (Unpublished). Available at [https://www.nbi.ku.dk/english/research/quantum-optics-and-photonics/theoretical-quantum-optics/studtheses/MSc\\_AntonLauenborgAndersen.pdf](https://www.nbi.ku.dk/english/research/quantum-optics-and-photonics/theoretical-quantum-optics/studtheses/MSc_AntonLauenborgAndersen.pdf)
- [Bha20] M. K. Bhaskar, R. Riedinger, B. Machielse, D. S. Levonian, C. T. Nguyen, E. N. Knall, H. Park, D. Englund, M. Loncar, D. D. Sukachev, *et al.*, *Nature* **580**, 60 (2020).
- [Bon15] K. Boone, J.-P. Bourgoin, E. Meyer-Scott, K. Heshami, T. Jennewein, and C. Simon, *Phys. Rev. A* **91**, 052325 (2015)
- [Bou14] J.-P. Bourgoin, E. Meyer-Scott, B. L. Higgins, B. Helou, C. Erven, H. Hübel, B. Kumar, D. Hudson, I. D'Souza, R. Girard, *et al.*, *New Journal of Physics* **16**, 069502 (2014)
- [Bra19] C. E. Bradley, J. Randall, M. H. Abobeih, R. C. Berrevoets, M. J. Degen, M. A. Bakker, M. Markham, D. J. Twitchen, and T. H. Taminiau, *Phys. Rev. X* **9**, 031045 (2019),
- [Col07] O. A. Collins, S. D. Jenkins, A. Kuzmich, and T. A. B. Kennedy, *Phys. Rev. Lett.* **98**, 060502 (2007)
- [Gün20] M. Gündogan, J. S. Sidhu, V. Henderson, L. Mazzarella, J. Wolters, D. K. L. Oi, and M. Krutzik, Arxiv: 2006.10636 (2020)
- [Kal17] N. Kalb, A. A. Reiserer, P. C. Humphreys, J. J. W. Bakermans, S. J. Kamerling, N. H. Nickerson, S. C. Benjamin, D. J. Twitchen, M. Markham, and R. Hanson, *Science* **356**, 928 (2017).
- [Pu17] Y.-F. Pu, N. Jiang, W. Chang, H.-X. Yang, C. Li, and L.-M. Duan, *Nature Communications* **8**, 15359 (2017)
- [Ren17] J.-G. Ren, P. Xu, H.-L. Yong, L. Zhang, S.-K. Liao, J. Yin, W.-Y. Liu, W.-Q. Cai, M. Yang, L. Li, *et al.*, *Nature* **549**, 70 (2017)
- [Wan17] Y. Wang, M. Um, J. Zhang, S. An, M. Lyu, J.-N. Zhang, L. M. Duan, D. Yum, and K. Kim, *Nature Photonics* **11**, 646 (2017).
- [Wit12] D. Witthaut, M. D. Lukin, and A. S. Sørensen, *Europhysics Letters* **97**, 50007 (2012),
- [Yin17] J. Yin, Y. Cao, Y.-H. Li, S.-K. Liao, L. Zhang, J.-G. Ren, W.-Q. Cai, W.-Y. Liu, B. Li, H. DaI *et al.*, *Science* **356**, 1140 (2017)